

# Collective Deceleration of Ultrarelativistic Nuclei and Creation of Quark-Gluon Plasma

I. N. Mishustin<sup>a,b,c</sup> and J. I. Kapusta<sup>a</sup>

<sup>a</sup>*School of Physics and Astronomy, University of Minnesota, Minneapolis, MN 55455, USA*

<sup>b</sup>*Niels Bohr Institute, Blegdamsvej 17, DK-2100 Copenhagen Ø, Denmark*

<sup>c</sup>*Kurchatov Institute, Russian Research Center, 123182 Moscow, Russia*

## Abstract

We propose a unified space-time picture of baryon stopping and quark-gluon plasma creation in ultrarelativistic heavy-ion collisions. It is assumed that the highly Lorentz contracted nuclei are decelerated by the coherent color field which is formed between them after they pass through each other. This process continues until the field is neutralized by the Schwinger mechanism. Conservation of energy and momentum allow us to calculate the energy losses of the nuclear slabs and the initial energy density of the quark-gluon plasma.

25.75.-q, 24.85.+p, 24.10.Jv, 12.38.Mh

Ultrarelativistic heavy-ion collisions offer a unique possibility to study collective dynamical effects at the partonic level. Before a collision the partons are confined in coherent field configurations and the Lorentz contracted nuclei can propagate in the physical vacuum without distortion. After the nuclei collide, thousands of partons are quickly liberated. The nuclei are transformed into two partonic sheets which recede from each other, leaving behind the perturbative QCD vacuum and strong gluon fields [1]. Since color charges on the sheets are distributed stochastically, they generate chromoelectric fields which are nonuniform in the transverse plane. This field configuration may be envisaged as a collection of densely packed color flux tubes or strings stretched between the sheets. The energy accumulated in the coherent field is taken from the kinetic energy of the receding partonic sheets that causes their deceleration. At later times the coherent fields are neutralized via the Schwinger pair-production mechanism [2].

In this letter we formulate a simple model to describe the collective deceleration of ultrarelativistic nuclei by the coherent color field. This model is similar in spirit to that proposed recently in ref. [3]. Some geometrical and kinematical aspects of the model are also similar to those introduced in ref. [4]. All calculations below are performed in the center-of-rapidity frame where the colliding nuclei have initial rapidities of  $\pm y_0$ .

We consider only beam energies so great that the nuclei can be thought of as very thin, Lorentz contracted, sheets. Each sheet is divided into many small elements, “slabs”, of unit transverse area labeled by an index  $a$  where  $a = p$  for the projectile nucleus and  $a = t$  for the target nucleus. Each slab is characterized by a baryon number  $N_a$  which is assumed to be strictly conserved. This number can be expressed through the slab thickness,  $l_a$ , in the rest frame of the respective nucleus,

$$N_a(\mathbf{b}) = \rho_0 l_a(\mathbf{b}) = \int dz \rho_a(\mathbf{b}, z) , \quad (1)$$

where  $\rho_a(\mathbf{b}, z)$  is the density distribution in nucleus  $a$ ,  $\mathbf{b}$  is the position of the slab in the impact parameter plane, and  $\rho_0 \approx 0.15 \text{ fm}^{-3}$  is the equilibrium nuclear density. For a uniform density distribution  $l(b) = 2\sqrt{R^2 - b^2}$ , where  $R = r_0 A^{1/3}$  is the nuclear radius and

$r_0 = (4\pi\rho_0/3)^{-1/3} \approx 1.17$  fm. We assume that before and after nuclear overlap, which takes place at  $t = 0$ , each slab propagates as a rigid body along the beam axes  $z$ . The energy and momentum of slab  $a$  is parameterized in terms of its proper energy per baryon  $\varepsilon_a$  and longitudinal rapidity  $y_a$  (for details see ref. [4]),

$$E_a = N_a \varepsilon_a \cosh y_a, \quad P_a = N_a \varepsilon_a \sinh y_a. \quad (2)$$

In general,  $\varepsilon_a$  may differ from the energy per baryon in normal nuclei,  $\varepsilon_0 \approx m_N$ , the nucleon mass, due to hard parton production at  $t = 0$ .

As a result of soft parton-parton interactions the slabs acquire color charges which generate the chromoelectric field or several strings in the space between them, see Fig. 1(a). For simplicity we disregard here a short time delay which is needed for the formation of the coherent field. At  $t > 0$  the trajectories of the projectile and target slabs,  $z_p(t)$  and  $z_t(t)$ , are affected by the energy and momentum losses for stretching the strings. If the string tension (energy per unit length) for individual strings is  $\sigma$ , and the number of strings per unit transverse area is  $n$ , then the potential energy stored in strings is  $V(z) = n\sigma|z_p - z_t|$  (for definiteness we assume that  $z_p > z_t$ ). Accordingly the force or, in the present context, the longitudinal pressure exerted by strings on slab  $a$  is  $-\partial V/\partial z_a = \mp n\sigma$ , and therefore Newton's equation of motion has the form

$$\frac{dP_a}{dt} = \mp n\sigma. \quad (3)$$

From here on the upper and lower signs correspond to  $a = p$  and  $a = t$ , respectively. The net force acting on both slabs is of course zero and the total energy of the slabs+field system is conserved. Realizing that the energy lost by a slab while traversing distance  $dz_a$  is equal to  $\mp n\sigma dz_a$ , one can also write the energy conservation equation as

$$\frac{dE_a}{dz_a} = \mp n\sigma. \quad (4)$$

These equations are identical to those describing the motion of massive capacitor plates due to the action of a uniform (chromo)electric field of a capacitor. This is not surprising

because the action of many collinear flux tubes, or strings, is equivalent to the action of a uniform field  $\mathbf{E}$  with the same energy density,  $\epsilon_f = \mathbf{E}^2/2 = n\sigma$ . It is important to note that  $\epsilon_f$  is a Lorentz invariant quantity.

Using eqs. (3) and (4) and the definition of slab velocity,

$$v_a = \frac{dz_a}{dt} = \frac{P_a}{E_a}, \quad (5)$$

one finds that  $P_a dP_a = E_a dE_a$ . This means that the internal energies of the slabs do not change in the course of deceleration, that is  $E_a^2 - P_a^2 = N_a^2 \epsilon_a^2 = \text{constant}$ . The solution to equations (3) and (4) for the initial condition  $y_a(0) = \pm y_0$ ,  $z_a(0) = 0$  are easily found to be:

$$\sinh y_a = \pm \left( \sinh y_0 - \frac{t}{\lambda_a} \right), \quad (6)$$

$$\cosh y_a = \cosh y_0 \mp \frac{z_a}{\lambda_a}, \quad (7)$$

where  $\lambda_a = (\epsilon_a \rho_0 / \epsilon_f) l_a$  is the characteristic deceleration length.

Eliminating  $y_a$  from these equations one obtains the slab trajectories

$$\left( \cosh y_0 \mp \frac{z_a}{\lambda_a} \right)^2 - \left( \sinh y_0 - \frac{t}{\lambda_a} \right)^2 = 1. \quad (8)$$

These are parts of hyperbolae shown in Fig. 2. Initially the slab trajectories are very close to the light cone but later on they increasingly deviate from it. If nothing else were to happen, the slabs would reach their respective turning points at  $t = \lambda_a \sinh y_0$ ,  $z = \pm \lambda_a (\cosh y_0 - 1)$ , and then reverse direction. As an example, Fig. 2(b) shoes the projectile trajectory with a turning point. This is the ‘‘yo-yo’’ type of motion well known in string models. However, such dynamics is very unlikely in nuclear collisions because of irreversible processes associated with string decay.

When the strings become long enough quark-antiquark and gluon pairs can be produced from vacuum via the Schwinger mechanism [2]. Their color charges will screen the chromo-electric fields and eventually neutralize them. For various idealized situations these processes were studied intensively during the last decade [5]. Here we want to avoid numerical simulations of the complicated plasma-field dynamics, which is not very well understood yet.

Instead we adopt a simplified picture assuming that the strings decay suddenly at a certain proper time  $\tau = \tau_0 \sim 1$  fm, where  $\tau = \sqrt{t^2 - z^2}$ . As a result, the partonic plasma is created at the hyperbola  $\tau = \tau_0$  (see Fig. 2). As we will see below, even this simplified picture allows us to make nontrivial predictions concerning the energy density and velocity field of the plasma at  $\tau = \tau_0$ .

As shown in Fig. 1(b), the structure of the system changes dramatically at  $t > \tau_0$ . Now the chromoelectric fields are absent in the middle but still remain in the regions adjacent to the projectile and target slabs. The gap between these two regions is filled by the partonic plasma. As time progresses the boundaries between the plasma and coherent fields move closer to the slabs, and the gap expands. Since in a time interval  $dt$  the boundaries traverse a distance  $dz$  along the hyperbola  $\sqrt{t^2 - z^2} = \tau_0$ , their velocities are  $dz/dt = t/\sqrt{t^2 - \tau_0^2} > 1$ . Although this velocity is superluminal, it has no physical significance since the boundary is not a material object. The plasma itself moves in accordance with the laws of special relativity. To see this, let us write the energy-momentum tensor of the plasma in the standard form

$$T^{\mu\nu} = (\epsilon + p)u^\mu u^\nu - pg^{\mu\nu} , \quad (9)$$

where  $\epsilon$  and  $p$  are the proper energy density and pressure,  $u^\mu$  is the collective 4-velocity of the plasma, and  $g^{\mu\nu} = \text{diag}(1, -1, -1, -1)$ . At its creation the plasma is assumed to have negligible transverse velocity; collective transverse expansion develops at later times. Thus the 4-velocity can be chosen as  $u^\mu = \gamma(1, 0, 0, v)$  where  $v$  is the longitudinal velocity and  $\gamma = 1/\sqrt{1 - v^2}$ . Now we can write equations expressing the conservation of energy and momentum across the boundary between the plasma and the chromoelectric field. In time  $dt$ , when the boundary moves a distance  $dz$ , the energy per unit area subtracted from the field is  $\epsilon_f dz$ . This change must be equal to the energy of a newly produced plasma slice  $dz$ :  $T^{00} dz = \epsilon_f dz$ . Using eq. (9) this gives

$$(\epsilon + p)\gamma^2 - p = \epsilon_f . \quad (10)$$

Since the field exerts a force  $n\sigma = \epsilon_f$  on the plasma charges, the change of momentum in the plasma slice  $dz$  is  $T^{03}dz = \epsilon_f dt$ . This leads to

$$(\epsilon + p)\gamma^2 v = \epsilon_f \frac{dt}{dz} = \epsilon_f \frac{z}{t} . \quad (11)$$

In the last equality we have used the condition that the boundary moves along the hyperbola  $\sqrt{t^2 - z^2} = \tau_0$  so that  $t dt = z dz$ . The two equations (10) and (11) allow us to find two quantities,  $\epsilon$  and  $v$ , characterizing the plasma at  $\tau = \tau_0$ . Especially simple results are obtained in the case of free streaming,  $p = 0$  (dust equation of state), which seems most appropriate for the early stages of the plasma evolution. By dividing eq. (11) by eq. (10) we get

$$v(\sqrt{t^2 - z^2} = \tau_0) = \frac{z}{t} = \tan \eta , \quad (12)$$

$$\epsilon(\sqrt{t^2 - z^2} = \tau_0) = \frac{\epsilon_f}{\gamma^2} = \frac{\epsilon_f}{\cosh^2 \eta} , \quad (13)$$

where the space-time (pseudo)rapidity  $\eta = \frac{1}{2} \ln \left( \frac{t+z}{t-z} \right)$  has been introduced. The first formula gives exactly the velocity field postulated in Bjorken's scaling hydrodynamics [6], but here it follows from the conservation laws at the plasma boundary. The second equation shows that it is the global energy-density  $T^{00} = \epsilon\gamma^2$  and not the rest-frame energy density  $\epsilon$  which should be constant at the hypersurface  $\tau = \tau_0$  where the plasma is created. As follows from eq. (13) the actual proper energy density at  $\tau = \tau_0$  decreases rather rapidly when going away from the central point  $\eta = 0$ . These predictions should be used as the initial conditions for further kinetic or hydrodynamical simulations of the plasma evolution.

The trajectories of the projectile and target slabs are not affected by the string decay until they intersect the hyperbola  $\tau = \tau_0$ . It is clear from the previous discussion that the region occupied by the plasma expands faster than the receding slabs. Thus the plasma eventually eats up the strings at time  $t_a^*$  when the slab trajectories intersect with the hyperbola  $\tau = \tau_0$ , as shown in Fig. 2. At this time the chromoelectric fields are fully neutralized and no new plasma is produced any more (see Fig. 1(c)). Substituting  $z_a^* = z_a(t_a^*)$  in eq. (7) we obtain the final gamma-factors and rapidities of the slabs,

$$\gamma_a^* = \cosh y_a^* = \gamma_0 \left[ 1 - \frac{\tau_0}{\lambda_a} \left( v_0 \sqrt{1 + \frac{\tau_0^2}{4\lambda_a^2}} - \frac{\tau_0}{2\lambda_a} \right) \right], \quad (14)$$

where  $\gamma_0 = \cosh y_0$  and  $v_0 = \tanh y_0$ . We see that  $\gamma_a^*$  is entirely determined by a single combination of parameters,  $\tau_0/\lambda_a = (\epsilon_f \tau_0)/(\epsilon_a \rho_0 l_a)$ . Since  $\epsilon_a \simeq m_N$  is not expected to vary much in the course of the reaction and  $l_a$  is given by the geometry, the combination  $\epsilon_f \tau_0$  is the only essential parameter of the model which determines the rapidity loss by the nuclei. It is quite natural that this is the same quantity which gives the initial transverse energy of the plasma at central pseudorapidity  $\eta = 0$ . As follows from eq. (13), the energy density of the plasma at  $\eta = 0$  and  $\tau = \tau_0$  is equal to  $\epsilon_f$ . The total energy of the plasma in a slice  $dz = \tau_0 d\eta$  around  $\eta = 0$  is obtained by integrating  $\epsilon_f(\mathbf{b})$  over transverse area of the reaction zone. This gives for central collisions

$$\frac{dE_T}{d\eta}(\eta = 0) = \pi R^2 \langle \epsilon_f \rangle \tau_0, \quad (15)$$

where  $\langle \epsilon_f \rangle$  is the energy density of the chromoelectric field averaged over the transverse area.

As our estimates show, it is most likely that  $\lambda_a \ll \tau_0$ . In this case the partonic slabs are significantly moderated at the time  $t_a^*$ . Indeed, in this limit  $t_a^* \approx z_a^* \approx \lambda_a \gamma_0$ , which is close to the turning point. From eq. (14) the condition of complete stopping ( $\gamma^* = 1$ ) is  $\tau_0/\lambda_a = \sqrt{2(\gamma_0 - 1)}$ . In collisions of asymmetric slabs the shorter slab may even reverse its motion in the direction of the longer slab, as illustrated in Fig. 2(b). Therefore, the proposed scenario provides an efficient mechanism for baryon stopping in ultrarelativistic heavy-ion collisions<sup>1</sup>. The baryon rapidity distribution is obtained by summing up contributions of all pairs of slabs and integrating over impact parameters. Our prediction is that in the first approximation this will be a superposition of two peaks centered at rapidities  $y_p^*$  and  $y_t^*$  given by eq. (14). In a more refined approach one should also study what happens to the baryonic slabs after they are hit by the plasma. It is clear that the plasma wind will cause

---

<sup>1</sup> One should keep in mind, however, that even in the case of complete stopping the projectile and target slabs will be separated in space by a distance of about  $(\lambda_p + \lambda_t)\gamma_0$ .

drift and diffusion of the baryon charge in rapidity space. As a result the projectile and target peaks will be shifted towards initial rapidities and smeared out.

The process of plasma creation described above is similar to the breakdown of a dielectric in a strong electric field. The electromagnetic plasma produced in this case shows up as a spark or lightning. Since here we are dealing with the QCD plasma, this phenomenon can be referred to as “QCD lightning”.

A direct calculation of the energy density  $\epsilon_f$  accumulated in the chromoelectric field at the early stage of a heavy-ion collision is problematic at present. Therefore, for our estimates we use a simple parameterization which is motivated by several model calculations.

$$\epsilon_f = \epsilon_0 \left( \frac{s}{s_0} \right)^{\alpha/2} \left( \frac{N_p N_t}{N_0^2} \right)^\beta . \quad (16)$$

Here the second factor is responsible for the incident energy dependence,  $\sqrt{s}$  is the c.m. collision energy per nucleon pair. The exponent  $\alpha \simeq 0.3$  follows from the low- $x$  behavior of the nuclear structure function or parton density [7]. The third factor accounts for the geometry of the overlap zone. The exponent  $\beta$  relates the number of strings produced to the number of binary parton-parton collisions, which is proportional to  $N_p N_t$ . For convenience we have normalized  $N_p$  and  $N_t$  by the mean areal baryon density in the proton,  $N_0 \approx 0.5 \text{ fm}^{-2}$ . In the case of uncorrelated strings, as in elementary pp or  $p\bar{p}$  collisions  $\beta \approx 1$ , while in the case of strong string overlap or percolation  $\beta \approx 0.5$  [8]. For the estimates below we use the value  $\beta = 0.5$ , also used in ref. [3], which seems appropriate for heavy-ion collisions at RHIC and LHC energies. It is assumed that this parameterization applies above a certain c.m. energy squared,  $s \geq s_0$ . The parameter  $\epsilon_0$  can be determined at  $s = s_0$  and then used for higher energies. With this choice we get

$$\frac{\tau_0}{\lambda_a} = \frac{\epsilon_f \tau_0}{\epsilon_a \rho_0 l_a} \propto \left( \frac{s}{s_0} \right)^{\alpha/2} \sqrt{\frac{l_{\tilde{a}}}{l_a}} , \quad (17)$$

where  $\tilde{a} = t$  for  $a = p$  and vice versa. This formula shows that in an asymmetric slab-slab collision ( $l_a < l_{\tilde{a}}$ ) the smaller slab will decelerate faster than the bigger one. This is a natural result since according to eq. (4) their energy losses are equal. For equal slabs



( $l_p = l_t = l$ ) the deceleration constant is independent of their lengths. This means that in a central collision the whole partonic sheet will decelerate uniformly. On the other hand, according to eq. (16), the energy density of the chromoelectric field decreases when going from the symmetry axis to the periphery,  $\epsilon_f(\mathbf{b}) \propto l(\mathbf{b})$ .

We shall now discuss phenomenological implications of our model in light of recent RHIC data for central Au+Au collisions at  $\sqrt{s} = 130$  GeV ( $y_0 = 4.94$ ). As found by the PHENIX collaboration [9], the transverse energy in the central pseudorapidity window is  $dE_T/d\eta|_{\eta=0} \approx 600$  GeV. For the free streaming plasma ( $p = 0$ )  $\epsilon(\tau)\tau = \epsilon(\tau_0)\tau_0$ , and  $dE_T/d\eta|_{\eta=0}$  is independent of  $\tau$ . Then from eq. (15) with  $\pi R^2 = 148$  fm<sup>2</sup> we immediately obtain  $\langle \epsilon_f \rangle \tau_0 \approx 3.9$  GeV/fm<sup>2</sup>. If the pressure effects are fully included,  $p = \epsilon/3$ , the transverse energy drops as  $\tau^{-1/3}$ , and in order to obtain the observed  $dE_T/d\eta$  one should increase the initial value by a factor  $(\tau_f/\tau_0)^{1/3} \simeq 2$ , where  $\tau_0$  and  $\tau_f$  are the initial and final time of hydrodynamic expansion. In our estimates we take for  $\langle \epsilon_f \rangle \tau_0$  the value 6 GeV/fm<sup>2</sup> which is in between these two extremes. This value is in qualitative agreement with results of microscopic simulations within the Quark-Gluon-String Model [10].

Now we can estimate the final rapidities of Au nuclei by considering the collision of representative slabs with lengths  $l_p = l_t = \langle l \rangle = 4R/3$  averaged over the transverse plane. Below we omit index  $a$  for simplicity. The proper energy per baryon in partonic slabs can be approximated by  $m_T = \sqrt{m_N^2 + \langle p_T \rangle^2}$ , where  $\langle p_T \rangle \approx 0.5$  GeV/c as measured by the STAR Collaboration [11]. To ensure energy conservation at  $t = 0$  we have reduced  $\gamma_0$  by the factor  $m_N/m_T$ . With these inputs we find from eq. (17) that  $\tau_0/\lambda = 4.1$  or the characteristic deceleration length  $\lambda = 0.24\tau_0$ <sup>2</sup>. From eq. (14) we get the final projectile and target rapidities,  $y^* \approx \pm 1.9$ . This corresponds to the final c.m. energy of about 3.5 GeV per baryon compared to the initial energy of 65 GeV per nucleon. The difference is transferred

---

<sup>2</sup>It is interesting to note that with  $\tau_0 = 1$  fm this would correspond to the total deceleration time and distance  $t^* \approx z^* \approx 14$  fm.

into the quark-gluon plasma. This is a tremendous energy loss which can explain the rather high degree of baryon stopping observed at RHIC. Unfortunately, the net-baryon rapidity distributions for this reaction are not available yet. Preliminary BRAHMS data show that the net-proton rapidity distribution has a dip at  $y = 0$  and two peaks at  $y = \pm(2 \div 3)$  [12].

Finally we use eq. (16) to make predictions for the full RHIC energy  $\sqrt{s} = 200$  GeV. Extrapolating from  $\sqrt{s} = 130$  GeV to  $\sqrt{s} = 200$  GeV, we get  $\langle\epsilon_f\rangle\tau_0 = 6.8$  GeV/fm<sup>2</sup> and  $y^* = \pm 2.1$ . If instead we would use the values  $\epsilon(\tau_0) = 66.5$  GeV/fm<sup>3</sup> and  $\tau_0 = 0.3$  fm given in ref. [13], we would predict that the baryonic slabs reach the turning point and reverse the direction of motion. Strict correlation between the transverse energy produced at central rapidities and the degree of baryon stopping is the most important prediction of our approach. The predicted strong deceleration of the baryon as well as the electric charge of ultrarelativistic nuclei makes it very promising to search for photon bremsstrahlung at collider energies (see ref. [14] and references therein).

In conclusion, the collective dynamics of partonic slabs has been studied within a simple model incorporating strong chromoelectric fields generated early in the reaction. The model has two essential physical parameters: the energy density accumulated in the chromoelectric field,  $\epsilon_f$ , and the proper time required for its neutralization,  $\tau_0$ . Applying conservation of energy and momentum, we have established a direct correspondence between the rapidity shifts of the projectile and target nuclei and the transverse energy of the produced quark-gluon plasma. Using data from recent RHIC experiments we have estimated the energy density accumulated in the chromoelectric field and the resulting rapidity shift in the net baryon distribution.

The authors thank P. J. Ellis and L. M. Satarov for useful discussions. I. N. M. acknowledges the kind hospitality of the Nuclear Theory Group, University of Minnesota. This research was supported by the Department of Energy under grant DE-FG02-87ER40328.

## REFERENCES

- [1] A. Kovner, L. McLerran, and H. Weigert, Phys. Rev. C **52**, 3809 (1995); 6231 (1995).
- [2] A. Casher, H. Neuberger, and S. Nussinov, Phys. Rev. D **20**, 179 (1979); N. K. Glendenning and T. Matsui, Nucl. Phys. **B245**, 449 (1984); K. Kajantie and T. Matsui, Phys. Lett. **164B**, 373 (1985); M. Gyulassy and A. Iwazaki, Phys. Lett. **165B**, 157 (1985).
- [3] V. K. Magas, L. P. Csernai, and D. D. Strottman, Phys. Rev. C, **64**, 014901 (2001).
- [4] Yu. B. Ivanov, I. N. Mishustin, and L. M. Satarov, Nucl. Phys. **A433**, 713 (1985).
- [5] G. Gatoff, A. K. Kerman, and T. Matsui, Phys. Rev. D **36**, 114 (1987); K. J. Eskola and M. Gyulassy, Phys. Rev. C **47**, 2329 (1993); F. Cooper, J. M. Eisenberg, Y. Kluger, E. Mottola, and B. Svetitsky, Phys. Rev. D **51**, 190 (1993); R. S. Bhalerao and G. C. Nayak, Phys. Rev. C **61**, 054907 (2000); D. V. Vinnik, A. V. Prozorkevich, S. A. Smolyansky, V. D. Toneev, M. B. Hecht, C. D. Roberts, and S. M. Schmidt, nucl-th/0103073.
- [6] J. D. Bjorken, Phys. Rev. D **27**, 140 (1983).
- [7] D. Kharzeev and E. Levin, nucl-th/0108006.
- [8] M. A. Braun, F. del Moral, and C. Pajares, hep-ph/0105263.
- [9] K. Adcox *et al.*, PHENIX Collaboration, Phys. Rev. Lett. **87**, 052301 (2001).
- [10] N. S. Amelin, N. Armesto, C. Pajares, and D. Sousa, hep-ph/0103060.
- [11] C. Adler *et al.*, STAR Collaboration, Phys. Rev. Lett. **87**, 112303 (2001).
- [12] J.-J. Gaardhoje, private communication.
- [13] A. Krasnitz and R. Venugopalan, Phys. Rev. Lett. **84**, 4309 (2000).
- [14] S. M. H. Wong, L. Belkacem, J. I. Kapusta, S. A. Bass, M. Bleicher, and H. Stöcker, Phys. Rev. C **63**, 014903 (2000).

## FIGURES

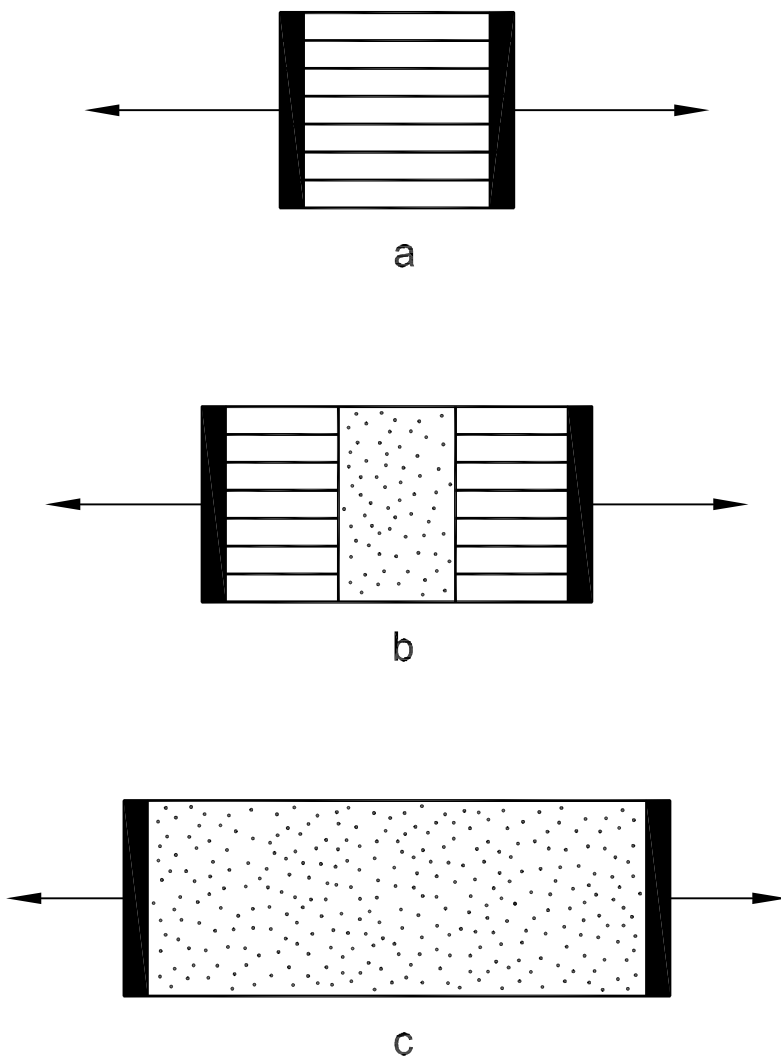


FIG. 1. Spatial view of a slab-slab collision at different times: (a)  $0 < t < \tau_0$ , (b)  $\tau_0 < t < t^*$  and (c)  $\tau \geq t^*$ . The black boxes represent the receding projectile and target slabs. The horizontal straight lines indicate strings. The dotted areas show the regions occupied by the quark-gluon plasma.

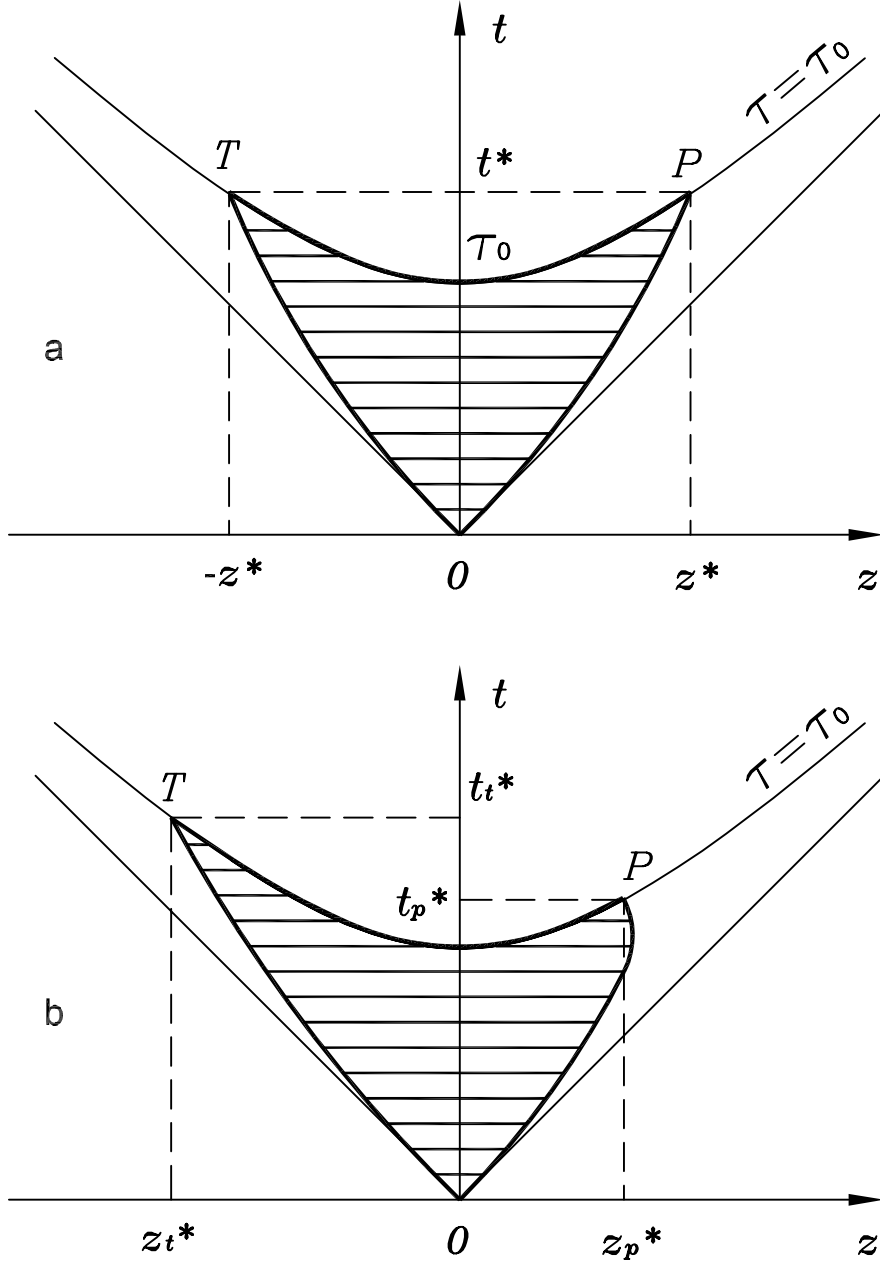


FIG. 2. Schematic space-time representation of a symmetric (a) and asymmetric (b) slab-slab collision in the  $t - z$  plane. The projectile and target slab trajectories are shown by thick solid lines which start at the origin and terminate at points  $P$  and  $T$ , respectively. The quark-gluon plasma is produced at the portion of the hyperbola  $\tau = \tau_0$  between these points (thick solid line). Horizontal solid lines represent strings. For symmetric collisions  $t_p^* = t_t^* = t^*$ ,  $z_p^* = -z_t^* = z^*$ .